Innovations in applied physics

Official English translation https://doi.org/10.18500/0869-6632-2019-27-1-77-95

Hyperbolic chaos in the Bonhoeffer–van der Pol oscillator with additional delayed feedback and periodically modulated excitation parameter

S. P. Kuznetsov, Yu. V. Sedova

Kotel'nikov's Institute of Radio-Engineering and Electronics of RAS, Saratov Branch
38, Zelenaya str., 410019 Saratov, Russia
E-mail: spkuz@yandex.ru, sedovayv@yandex.ru
Correspondence should be addressed to Sedova Yuliya V., sedovayv@yandex.ru
Received 13.10.2018, accepted for publication 3.12.2018

Topic and aim. The aim of the work is to consider an easy-to-implement system demonstrating the Smale–Williams hyperbolic attractor based on the Bonhoeffer–van der Pol oscillator, alternately manifesting a state of activity or suppression due to periodic modulation of the parameter by an external control signal, and supplemented with a delayed feedback circuit. **Investigated models.** A mathematical model is formulated as a non-autonomous second-order equation with delay. A scheme of the electronic device that implements this type of chaotic behavior is proposed. **Results.** The results of numerical simulating of the system dynamics, including waveforms, oscillation spectra, plots of Lyapunov exponents, a chart of regimes on the parameters plane are presented. The circuit simulation of the electronic device using the software Multisim is carried out. **Discussion.** The Smale–Williams attractor in the system appears due to the fact that the transformation of the phases of the carrier for the sequence of radio-pulses generated by the system corresponds to a circle map expanding by an integer factor. The important feature of the system is that the transfer of excitation from one to the next stage of activity with doubling (or tripling) of the phase occurs due to the resonance mechanism involving a harmonic of the developed oscillations that have twice (or triple) longer period than that of small oscillations. Due to the hyperbolic nature of the attractor, the generated chaos is rough, that is, it is characterized by low sensitivity to variations in the parameters of the device and its components. Our scheme corresponds to a low-frequency device, but it can be adapted for chaos generators also at high and ultrahigh frequencies.

Key words: dynamical system, time-delay, chaos generator, attractor, Lyapunov exponent, circuit simulation.

Reference: Kuznetsov S.P., Sedova Yu.V. Hyperbolic chaos in the Bonhoeffer–van der Pol oscillator with additional delayed feedback and periodically modulated excitation parameter. *Izvestiya VUZ. Applied Nonlinear Dynamics*, 2019, vol. 27, no. 1, pp. 77–95. https://doi.org/10.18500/0869-6632-2019-27-1-77-95

Acknowledgements. Development of the operating principle of the system, construction of a mathematical model, numerical calculations and processing of the results are supported by the grant of Russian Science Foundation № 17-12-01008 (sections 1, 2). The development of electronic devices and circuit simulation in environment Multisim is executed with support of Russian Foundation for Basic Research grant № 16-02-00135 (section 3).

Introduction

Construction of different variants of coupled systems based on self-oscillating elements described by the Bonhoeffer–van der Pol equations, including systems with delayed feedbacks, is of interest for many reasons. First, the Bonhoeffer–van der Pol oscillator can be easily implemented in the form of an electronic circuit and in combined circuits that demonstrate complex dynamics. At the same time it can serve as a basis for constructing signal generators with wide functional capabilities. Secondly, as the Bonhoeffer–van der Pol equation corresponds to the well-known FitzHugh–Nagumo neuron model up to replacement of the variables [1–5], we can speak about the application of such systems for model description of the phenomena taking place in neurosystems, and about analog simulation of these phenomena using electronic circuits. Third, the proposed study contributes to the development of examples of dynamical behavior that are known in the modern theory of dynamical systems on the level of abstract mathematical representations, but are still awaiting detection and application in real-world systems. This field of research may open up the possibility of building technical devices that reproduce the properties of natural neurosystems, as well as generators of rough chaos, insensitive to variations in the parameters of the device and its components.

The uniformly hyperbolic attractors taken into consideration according to the mathematical theory developed in the 1960–1970s, serve as a strictly justified example of deterministic chaos in dynamical systems [6–13]. These are attractors composed exclusively of saddle-type phase trajectories, the characteristic feature of which is that each trajectory on the attractor has many neighboring trajectories approaching it and many other trajectories moving away from it (stable and unstable manifolds).

The fundamental mathematical fact is that hyperbolic chaos has the property of roughness, or structural stability. In the theory of oscillations, it is customary to postulate that rough systems showing motions that do not change qualitatively with slight variation of parameters [14–16] should be of interest from both theoretical and practical point of view. This property seems to be extremely important for natural systems and technical applications, since it ensures insensitivity of the chaos characteristics in systems with hyperbolic attractors in respect to inaccurate parameter settings, manufacturing errors, various imperfections and disturbances.

An example of a hyperbolic attractor is the Smale–Williams solenoid [6–9]. Let us consider a region in the form of a torus in three-dimensional space and a map that stretches the torus twice with sufficiently strong transverse compression per one step of discrete time and folds it into a twice loop placed inside the original torus. At every next step of the transformation, the total volume of the object decreases (this means that the map is dissipative), and the number of turns doubles. In the limit of an infinite number of steps, this number tends to infinity, and the formation called solenoid appears, being a hyperbolic attractor. In the transverse direction, the solenoid has the structure of Cantor set. Similar construction can be made using longitudinal stretching not by factor two, but in a greater number of times $M = 3, 4, \ldots$ and folding of loops with the corresponding number of coils M, which complies with hyperbolic attractors in the form of solenoids of a different topological type.

As the theory of dynamical systems and its applications were developing, it turned out that numerous examples of chaotic dynamics, known in different fields of science and technology, do not satisfy the conditions of the hyperbolic theory. Only recently, physical examples of systems with structurally stable hyperbolic chaos have been proposed and implemented [17]. Several such examples are based on systems using delayed feedback [18–22].

The article describes a simple-to-implement system that demonstrates the Smale–Williams hyperbolic attractor, where the Bonhoeffer–van der Pol oscillator appears to be the main element, which is alternately in the state of excitation or suppression due to periodic modulation of the parameter by an external control signal and supplemented by a delayed feedback circuit. The attractor is hyperbolic

due to the fact that the transformation of the filling phases for the generated sequence of radio pulses corresponds to a circle map stretching an integer number of times. A feature of this system is that the excitation transfer from one stage of activity to another with phase doubling is carried out in a resonant manner at the harmonic of relaxation oscillations, the period of which is two or three times longer than that of small oscillations. A mathematical model is formulated, described by a non-autonomous second-order equation with a delayed argument, and the results of numerical simulation of the system dynamics, including waveforms, oscillation spectra, graphs of Lyapunov exponents, and a chart of regimes on the parameter plane are presented. The circuit of an electronic device that implements this type of chaotic behavior is suggested, and its dynamics is simulated using Multisim software product.

1. The Bonhoeffer–van der Pol oscillator. Weakly nonlinear and relaxation self-oscillations

The Bonhoeffer–van der Pol oscillator is a self-oscillating system described by the equation

$$\ddot{x} - (A - x^2)\dot{x} + x = K. \tag{1}$$

When parameter A has small positive values, approximately sinusoidal self-oscillations appear in the system with the frequency being close to $\omega = 1$. When A increases, transition to relaxation oscillations, which substantially differ from the sinusoid, takes place, and the main frequency decreases. If parameter K is different from zero, then both odd and even harmonics are presented in the oscillation spectrum, while for the classical van der Pol oscillator, which corresponds to the case when $K = 0$, only odd harmonics are presented. Fig. 1 shows the portraits of attractors on the phase plane of equation (1) in the regimes of small quasi-harmonic oscillations and large, relaxation oscillations when $K = 0.5$. If parameter A is small, then the dimensionless circular oscillation frequency is close to 1. When $A = 5.5$ the fundamental frequency is approximately 1/2, and the second harmonic frequency is close to the frequency of small oscillations respectively. When $A = 9.66$, the fundamental frequency is approximately 1/3, and the frequency of the third harmonic is close to the frequency of small oscillations.

In Fig. 2, *a*, the resonance buildup of oscillations of the linear oscillator $\ddot{y} + y = \varepsilon x$ under the second harmonic of the self-oscillating system (1) according to numerical solution of the problem with parameters $A = 5.5$, $K = 0.5$, $\varepsilon = 0.1$ is illustrated. Visually, the period of oscillations of a linear oscillator is twice as large as the period of self-oscillations of the system (1), so that the frequency of

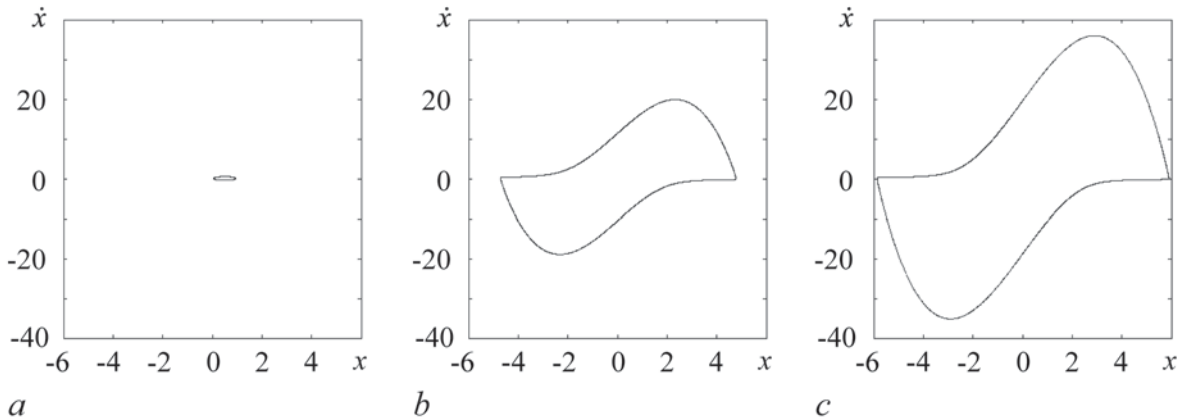

Fig. 1. Evolution of phase portraits for the model (1) in the case $K = 0.5$ for different values of the parameters: A=0.3 (*a*), oscillation frequency $\omega \approx 1$; A=5.5 (*b*), oscillation frequency $\omega \approx 1/2$; A=8.5 (*c*), oscillation frequency $\omega \approx 1/3$

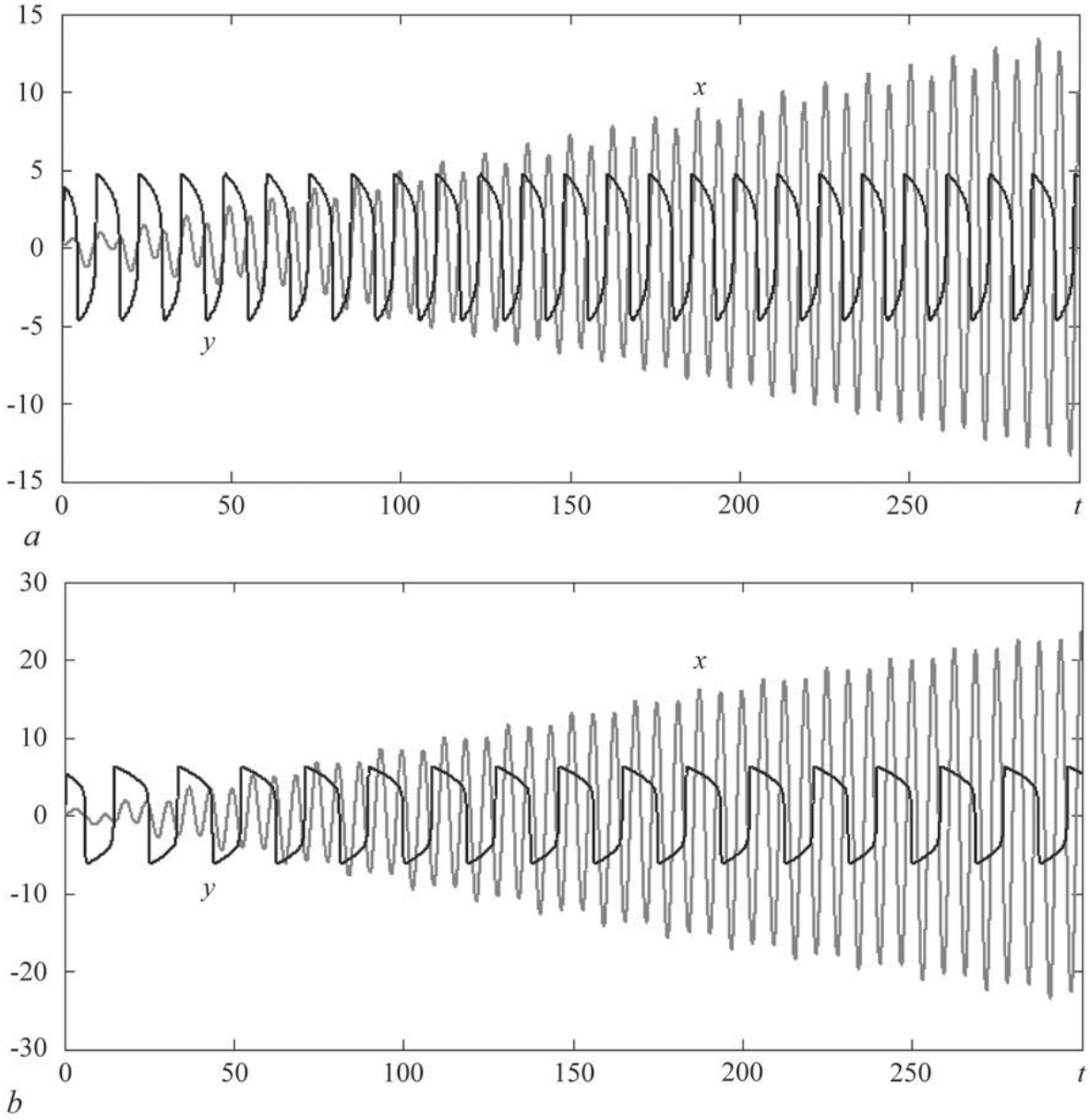

Fig. 2. Resonant excitation of a linear oscillator by the second (*a*) and the third (*b*) harmonics of the self-oscillating system as obtained from numerical solution of the set of equations $\ddot{x} - (A - x^2)\dot{x} + x = K$, $\ddot{y} + y = \varepsilon x$ at $K = 0.5$, $\varepsilon = 0.1$, $A = 5.5$ (*a*) and $A = 9.66$ (*b*)

the second harmonic of self-oscillations coincides with the natural frequency of the linear oscillator. A similar diagram in Fig. 2, *b* the resonant buildup of oscillations under the action of the third harmonic when $A = 9.66$ is shown.

In [23], the idea of using situations of an integer ratio of the frequencies of small and large oscillations with resonant excitation of oscillations by means of harmonics to construct a system with Smale–Williams type attractors based on two subsystems – weakly coupled Bonhoeffer–van der Pol oscillators, which alternate between activity or suppression due to modulation of the parameters controlling the excitation in antiphase for both subsystems was proposed.

In this case, the parameters are chosen so that at the stage of activity the relaxation oscillations have a period an integer number of times longer than the period of small oscillations. Due to the transfer of excitation alternately from one oscillator to another, the Smale–Williams attractors can be obtained with different values of the stretching factor of the angular variable in the phase space of the map describing the change of the state of the system during the modulation period, the angular variable being the phase of oscillations. A similar principle was used in [24] to construct a mechanical system with hyperbolic attractor based on the Froude pendulums with alternating braking.

In this paper we show that, introducing an additional delayed feedback circuit, it becomes possible to implement the Smale–Williams attractor in a system based on only one Bonhoeffer–van der Pol oscillator with parameter modulation. The corresponding electronic device turns out to be simpler and contains fewer components than the system based on two oscillators. From the point of view of the mathematical description and the theory of dynamical systems it is more complicated, because due to the presence of delay the phase space is infinite-dimensional.

2. Oscillator with additional delayed feedback and modulation of the excitation parameter

Let us consider the Bonhoeffer–van der Pol oscillator, where the control parameter slowly varies in time according to a periodic law, providing alternating excitation and damping of the oscillations, and additional delayed feedback is introduced. Let the parameter remain constant for some time at a stage of excitation and equal to the maximum value of a, then it decreases to the negative value $(-c)$, and then increases again, reaching the maximum value. We write the dynamical equations in the following form:

$$\ddot{x} - (f(t/T + 1/4) - x^2)\dot{x} + x = K + \varepsilon(x(t - \tau) - x), \tag{2}$$

where x is a dynamic variable, K is a parameter, ε is a coefficient characterizing the value of the delayed feedback, τ is the delay time. The function f determines the dependence on the time of the control parameter A and, on the period of its argument being one, is given by the following relations

$$f(\xi) = \begin{cases} a, \ 0 < \xi \le \tau_1, \\ \dfrac{(a-c)\xi + c\tau_1 - a\tau_2}{\tau_1 - \tau_2}, & \tau_1 < \xi \le \tau_2, \\ \dfrac{(c-a)\xi + a\tau_2 - c}{\tau_2 - 1}, & \tau_2 < \xi \le 1. \end{cases} \tag{3}$$

It is important to emphasize that the system with delay is characterized by an infinite dimension of phase space [25–28]. In fact, in order to indicate the condition that makes it possible to unambiguously determine the subsequent dynamics, it is necessary to specify not only the values x and $\dot{x}$ at the initial moment of time, but also the function $x(t - \tau)$ on the previous time interval of duration τ.

We can determine stroboscopic map of the system (2) (Poincaré map) for the modulation period T, introducing it formally as

$$\mathbf{X}_{n+1} = \mathbf{F}_T(\mathbf{X}_n), \tag{4}$$

where vector $\mathbf{X}_n$, which defines the system state at the moment $t_n = nT$, should be interpreted as an element of infinite-dimensional space in this case.

Let us explain the principle of the system functioning in the regime with hyperbolic attractor. At the stage of activity, the oscillator performs relaxation type self-oscillations. As the parameter a value being chosen appropriately, the main self-oscillation frequency appears to be an integer number

of times of M less than the frequency of small oscillations (particularly, we consider cases $M = 2$ and 3). During the attenuation stage, the oscillations practically disappear, but when the time for a new stage of activity comes, the appearance of oscillations is stimulated in a resonant manner by the Mth harmonic of the signal, which arrives from the delayed feedback circuit, having been emitted at the previous stage of the presence of developed relaxation oscillations of the oscillator. Therefore, the phase of these oscillations corresponds to the phase of the main component of the oscillations multiplied by the factor M. As a result, when the newly appearing oscillations of the oscillator reach the steady state of relaxation self-oscillations, their phase will correspond to the oscillation phase multiplied by the factor M in comparison with the phase at the previous stage of activity. Then the process repeats itself over and over again. Therefore, the expanding circle map takes place for phases of the oscillatory process at successive stages of activity. With compression in other directions in the phase space, this corresponds to formation of the Smale–Williams solenoid for the Poincaré map (4). In the problem under consideration, this solenoid is an object embedded in the infinite-dimensional phase space of the map (4).

Let us turn to illustrations of the functioning of the system, paying attention to the results of numerical simulation. The equations were solved using the Runge–Kutta method of the 4th order adapted for the system with delay. To do this, the current values of variables and functions at each step of the difference scheme are stored in the form of an array of data on the previous time interval τ, so that they can be used at the right time to perform calculations when it is necessary to substitute the delayed values of these quantities.

Figures 3 and 4 show the graphs of the time dependence for the variable x and its derivative over several periods of modulation for the case, when the transfer of excitation from the previous stage of activity to the next one is carried out at the second and third harmonics, respectively, for $a = 5.5$ and 9.66. The other parameters are

$$K = 0.5, \quad c = -2, \quad \tau_1 = 0.4, \quad \tau_2 = 0.5, \quad \varepsilon = 0.01, \quad T = 200, \quad \tau = T/2. \tag{5}$$

In order to make sure quantitatively, that there is a correspondence between the dynamics of the system during the modulation period and the procedure that determines formation of the Smale–Williams solenoids, we turn to the construction of diagrams of the phase dependences at the next stage of activity on the phase at the previous stage of activity. It should be noted that in the region of developed self-oscillations, the form of the oscillations differs significantly from the sinusoidal one, therefore, the calculation of the phases through arctangent of the ratio of the variable and its derivative leads to unsatisfactory results. An alternative is to use the value that determines the time shift relative to a given reference point, normalized to a characteristic period of oscillation. Let t be an initial moment of a stage of braking of the oscillator, t_1 and t_2 be the preceding moments of the oscillator passing through the section $x = 0$, where $t_2 > t_1$. Then it is possible to determine the angular (phase) variable which belongs to the interval [0,1] according to the relation $\varphi = (t - t_2)/(t_2 - t_1)$. The calculation of this quantity is easily programmed and is performed in the process of numerical simulation of the system dynamics.

The diagrams in Fig. 5, based on the results of numerical solution of equations (2) on a large number of modulation periods, illustrate the transformation of the oscillation phases in successive stages of activity in accordance with the twice-stretching circle map when $a = 5.5$ (*a*) and the triple-stretching map when $a = 9.66$ (*b*).

Fig. 6 shows portraits of attractors of stroboscopic map. These are two-dimensional projections of the Smale–Williams solenoids for the Poincaré map of our system with infinite-dimensional phase space. The intrinsic fractal transverse structure of fibers is indistinguishable here due to the high degree of transverse compression at every step of the map.

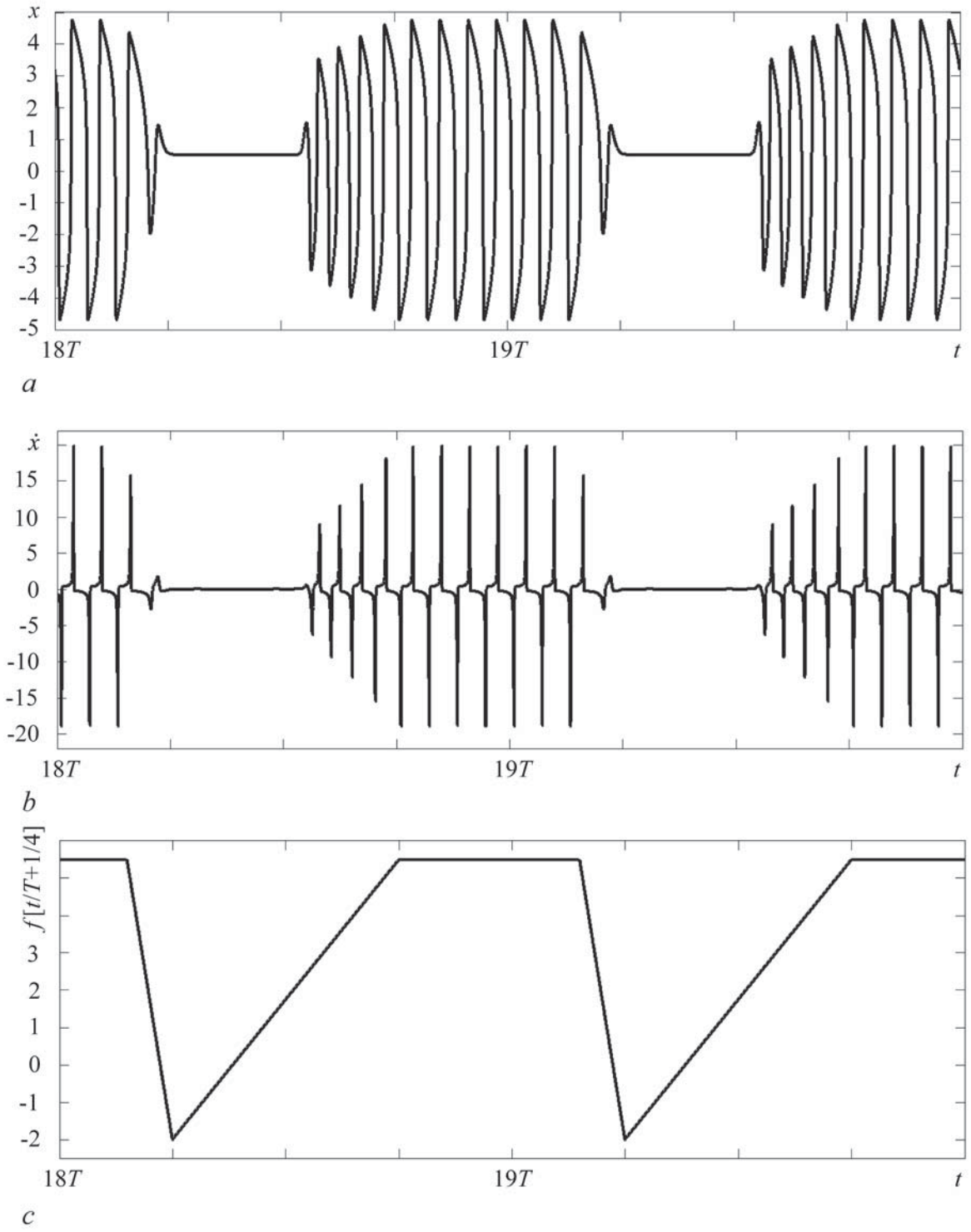

Fig. 3. *a*, *b* – waveforms $x(t)$ and $\dot{x}(t)$ of the system (2), $a = 5.5$, $K = 0.5$, $c = -2$, $\varepsilon = 0.01$, $T = 200$, $\tau = T/2$, $\tau_1 = 0.4$, $\tau_2 = 0.5$; *c* – the function f governing the modulation of the control parameter

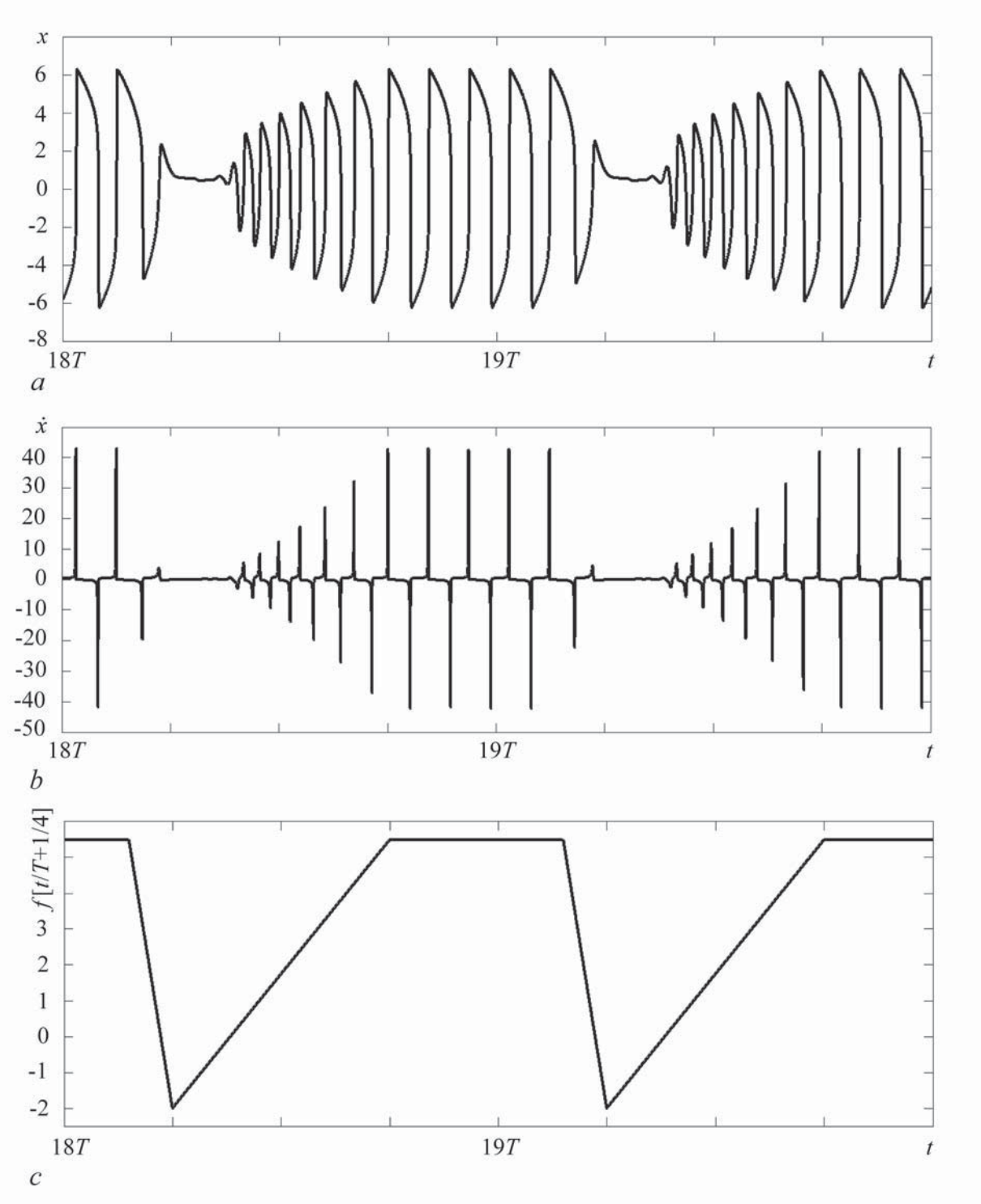

Fig. 4. *a*, *b* – waveforms $x(t)$ and $\dot{x}(t)$ of the system (2), $a = 9.66$, $K = 0.5$, $c = -2$, $\varepsilon = 0.01$, $T = 200$, $\tau = T/2$, $\tau_1 = 0.4$, $\tau_2 = 0.5$; *c* – the function f governing the modulation of the control parameter

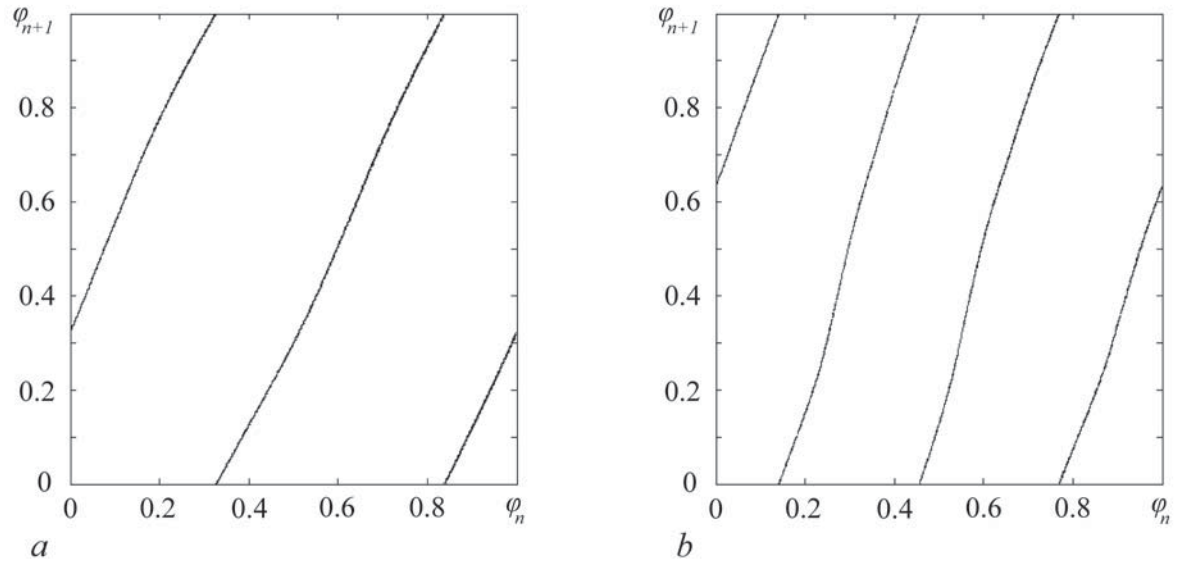

Fig. 5. Iteration diagrams for the oscillation phases of the system (2) at parameters $a = 5.5$ (*a*) and $a = 9.66$ (*b*). Other parameters are $K = 0.5$, $c = -2$, $\varepsilon = 0.01$, $T = 200$, $\tau = T/2$, $\tau_1 = 0.4$, $\tau_2 = 0.5$

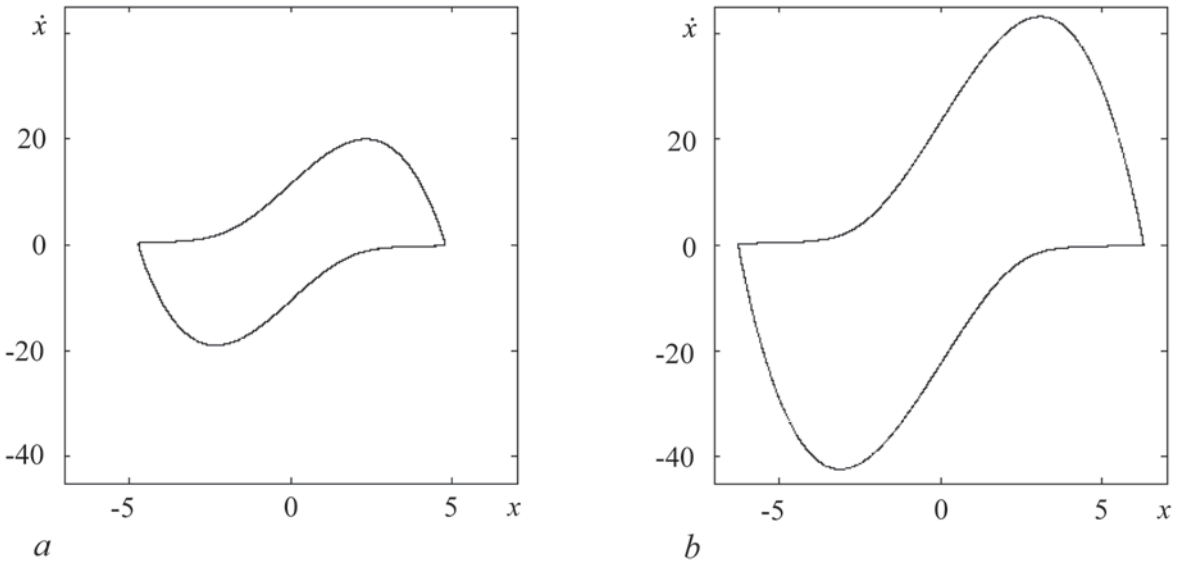

Fig. 6. Portraits of attractors of the Poincaré map over the modulation period in the projection onto a plane of variables $(x, \dot{x})$ at $a = 5.5$ (*a*) and $a = 9.66$ (*b*). Other parameters are $K = 0.5$, $c = -2$, $\varepsilon = 0.01$, $T = 200$, $\tau = T/2$, $\tau_1 = 0.4$, $\tau_2 = 0.5$

For the system with delay, the total number of Lyapunov exponents is infinite. Nevertheless, we can evaluate the first few exponents in descending order of their values within the Benettin technique adapted for a system with delay [27–30]. For this the numerical solution of the equation (2) is simultaneously performed together with the corresponding number of equations in variations

$$\ddot{\tilde{x}} - (f(t/T + 1/4) - x^2)\dot{\tilde{x}} + 2x\dot{x}\tilde{x} + \tilde{x} = \varepsilon(\tilde{x}(t - \tau) - \tilde{x}) \tag{6}$$

and with orthogonalization of the Gram–Schmidt perturbation vectors at each step of integration of the equations. (Note that the perturbation vector is specified by the function $\tilde{x}(t)$ on a finite interval equal to the delay time.) The Lyapunov exponents of the attractor shown in Fig. 6, *a*, for the map over a period are

$$\Lambda = \{\, 0.690,\ -7.950,\ -8.750,\ ...\}, \tag{7}$$

and the dimension of the attractor in the stroboscopic section according to Kaplan–Yorke is $D_{KY} = = 1 + \Lambda_1/|\Lambda_2| \approx 1.09$. For the attractor shown in Fig. 6, *b*, the Lyapunov exponents are

$$\Lambda = \{1.081,\ -8.642,\ -9.270,\ ...\}, \tag{8}$$

and the Kaplan–Yorke dimension is $D_{KY} = 1 + \Lambda_1/|\Lambda_2| \approx 1.13$.

Let us note that the positive Lyapunov exponent in the spectrum of exponents (7) is close to $\ln 2$, and in the spectrum of (8) it is close to $\ln 3$. This corresponds to an expanding circle map for phases at successive stages of activity, two or three times, respectively, which is consistent with the system functioning mechanism described above.

Figure 7 shows the dependence of three Lyapunov exponents on parameter a when the remaining parameters are fixed. It can be seen that in certain parameter intervals the largest Lyapunov exponent has the values corresponding to the stretching of the angular variable by 2 and 3 times. This corresponds to implementation of attractors in the system in the form of Smale–Williams type solenoids with double

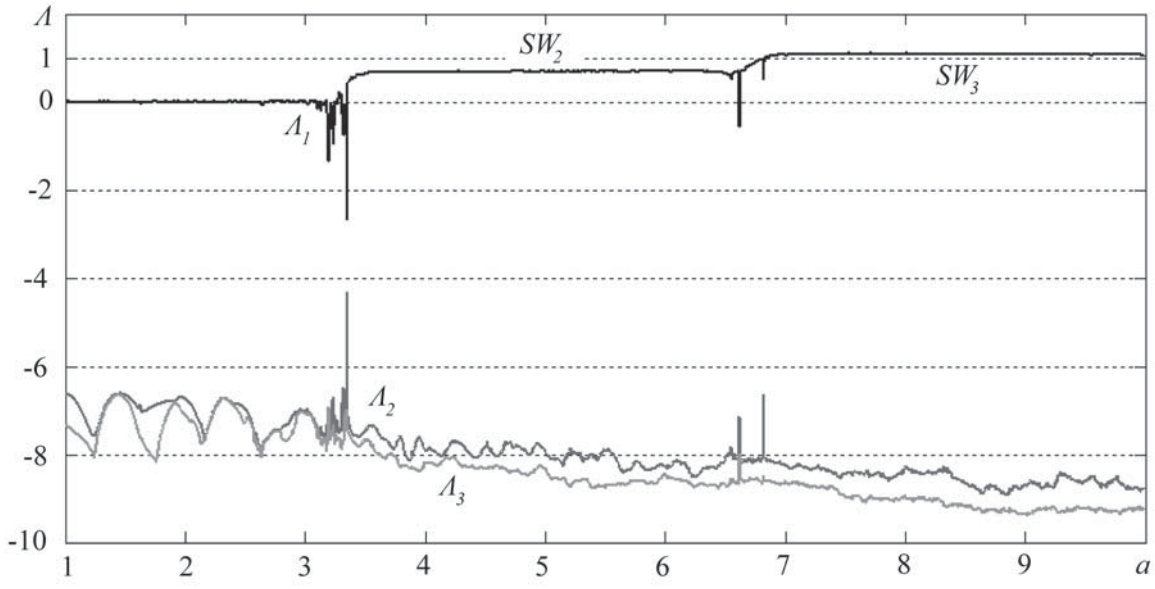

Fig. 7. The dependence of the largest three Lyapunov exponents of the system (2) on the parameter a. Other parameters: $K = 0.5$, $c = -2$, $\varepsilon = 0.01$, $T = 200$, $\tau = T/2$, $\tau_1 = 0.4$, $\tau_2 = 0.5$. The intervals corresponding to Smale–Williams attractors with double and triple expanding of the phase variable are indicated respectively by the labels SW_2 and SW_3

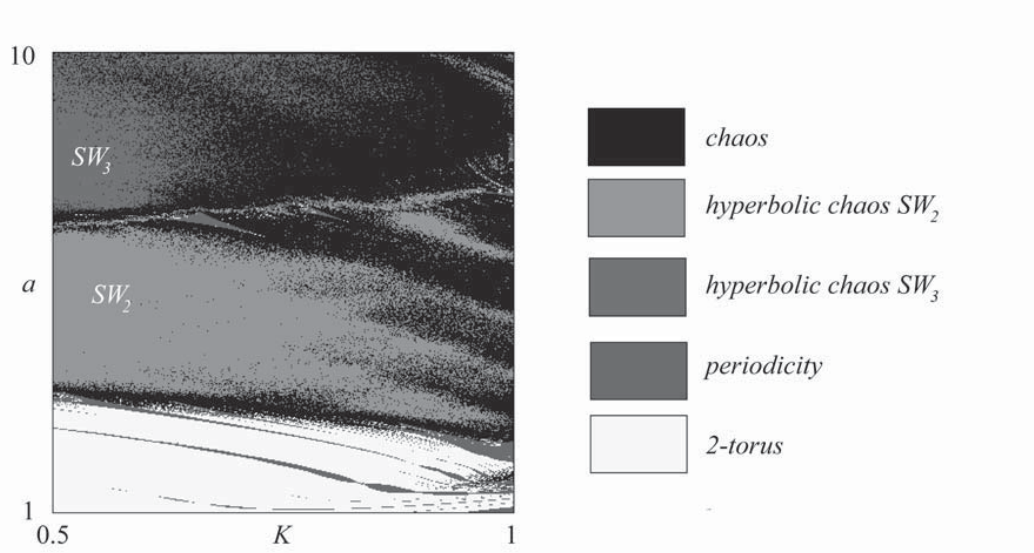

Fig. 8. Chart of regimes for the parameter plane (K, a) of the system (2), where areas of regimes, which are indicated by definite color and the corresponding inscriptions, are diagnosed by the values of Lyapunov exponents. The remaining parameters are $c = -2$, $\varepsilon = 0.01$, $T = 200$, $\tau = T/2$, $\tau_1 = 0.4$, $\tau_2 = 0.5$

or triple loop folding at one step of construction with sufficiently strong transverse compression, which is proved by presence of negative exponents quite large in absolute value. These intervals correspond to structurally stable hyperbolic chaos as a smooth nature indicates of the Lyapunov exponent dependence on the parameter. In the areas of transitions between the plateaus on the graph, one can see dips intrinsic to non-hyperbolic chaos, corresponding to periodicity windows.

Figure 8 shows a chart of regimes of the system (2) on the parameter plane (K, a). To construct it, a selected area along two coordinate axes on the grid with a small step was scanned. Each pixel is marked in color in accordance with the regime diagnosed at a given point that occurs during the numerical integration of equations. If all exponents are negative, then this corresponds to a regular periodic regime, namely, an attracting periodic point of the Poincaré map. The closeness of the largest exponent to zero indicates quasiperiodic dynamics, which in the phase space of the Poincaré map corresponds to an attractive closed invariant curve. The presence of a positive exponent shows the chaotic nature of attractor of the Poincaré map, which can be hyperbolic or non-hyperbolic.

While plotting the chart, the proximity of the positive Lyapunov exponent of the map for the modulation period to the value ln 2 or ln 3, corresponding to the double or triple stretching circle map, was taken as a sign of the occurrence of the hyperbolic Smale–Williams attractor. Check computations confirm that the hyperbolicity region is determined quite accurately with the help of this method: the form of the map built at the points of the found region, qualitatively corresponds to Fig. 5 (the graphs are composed of 2 or 3 branches). In accordance with its inherent property of structural stability, the hyperbolic chaos occupies continuous regions on the parameter plane, marked as SW2 and SW3.

Figure 9 shows power spectra of the signal generated by the system for both types of the Smale–Williams attractor SW2 and SW3 (with doubling and tripling the number of loops at the construction stage). The spectra were computed by means of processing time series for the dynamic variable x obtained by numerical integrating of the equations using the method of statistical estimation of the spectral density of random processes [31, 32].[1] It can be seen from the figure that in each of the

[1] To obtain a spectrum, the time series is divided into sections of a certain duration which exceeds the characteristic time scale of the signal, followed by multiplying a segment of the time series by the «window» function (to improve the quality

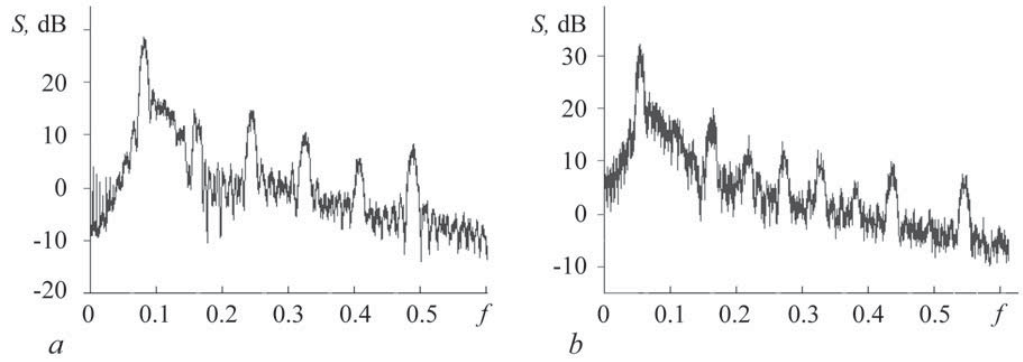

Fig. 9. The power density spectra of the signal $x(t)$ in logarithmic scale at $a = 5.5$ (*a*) and $a = 9.66$ (*b*). Other parameters: $K = 0.5$, $c = -2$, $\varepsilon = 0.01$, $T = 200$, $\tau = T/2$, $\tau_1 = 0.4$, $\tau_2 = 0.5$

cases taken into consideration the spectrum is continuous, the same as in random process although it is characterized by a noticeable indentation – the occurrence of blurry peaks due to the presence of correlations between waveforms at the intervals spaced by the delay time interval.

3. Electronic generator of rough chaos and its circuit simulation

Let us consider the circuit implementation of the above-described idea of obtaining hyperbolic chaos in a system where a self-oscillating element with alternating excitation and damping is supplemented by a delayed feedback circuit for transmitting excitation with phase doubling at the next stage of activity due to the use of the second harmonic of the resulting relaxation oscillations. Fig. 10 shows a circuit, the main element of which is an oscillator based on the oscillatory circuit L1C1. The introduction of negative resistance into the circuit is provided by the operational amplifier OA1. The value of introduced resistance at any specific time depends on the instantaneous source-drain resistance of the field-effect transistor Q1. The control voltage applied to the gate from the source V1 remains zero for a certain part of the modulation period (the oscillator is active), and the voltage is less than zero for the rest of the period (oscillations are suppressed), and time dependence of the voltage is expressed by a triangular function. The parameters of the negative resistance elements are chosen so that the zero gate voltage corresponds to arising relaxation oscillations with a frequency half of that for the linear oscillations.

The diode D1 is included into the oscillatory circuit, which ensures the limitation of the level of oscillations and the presence of intense second harmonic at large amplitudes of oscillations. When the next stage of oscillator activity begins, the development of the oscillations, which start with small amplitude, is effectively stimulated in a resonant manner because of the coupling through the capacitor C2 due to the second harmonic of the oscillations received through the delay line T from the previous stage of the developed relaxation oscillations. Since the transfer of excitation is carried out through the second harmonic, this should be accompanied by doubling of the phase, which, in the presence of compression in other directions in the state space, will correspond to an attractor of the Smale–Williams type in a stroboscopic map that determines the evolution of the system over a period.

Fig. 11 shows the waveforms obtained by simulation with the help of Multisim software, which demonstrate the operation of the circuit according to the above-described mechanism.

---

of spectral analysis due to suppression of the effect of signal mismatch at the edges of the partition intervals). Next, Fourier transform is performed on each section, and the squares of the amplitudes of the spectral components are averaged over the set of partition sections.

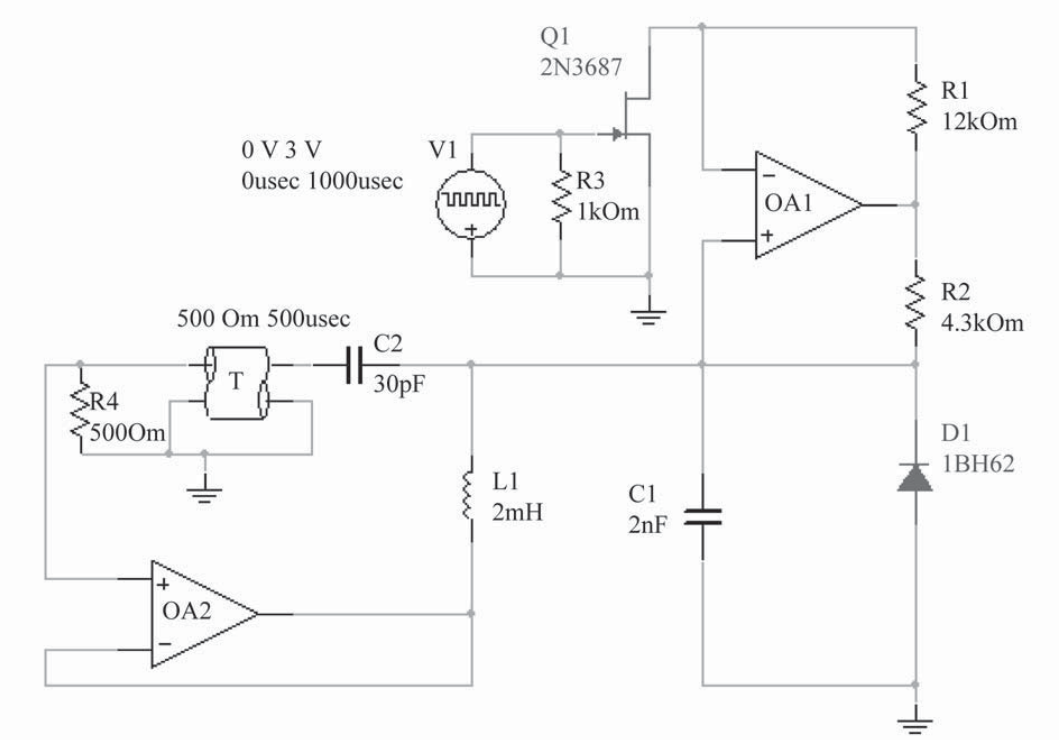

Fig. 10. Generator circuit with periodic excitation and delayed feedback, realizing hyperbolic chaos

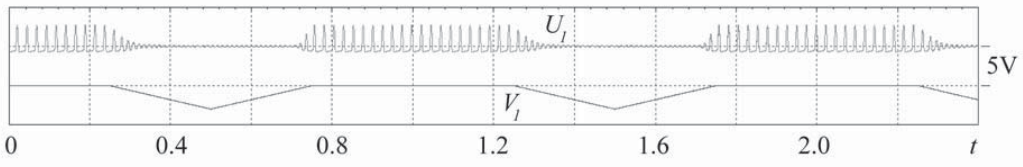

Fig. 11. Waveforms of voltages U_1 on capacitor C1 and control voltage V_1 on the gate of field effect transistor V1 obtained with the help of a virtual oscilloscope in the Multisim simulation. The nominal values of the circuit elements correspond to Fig. 10

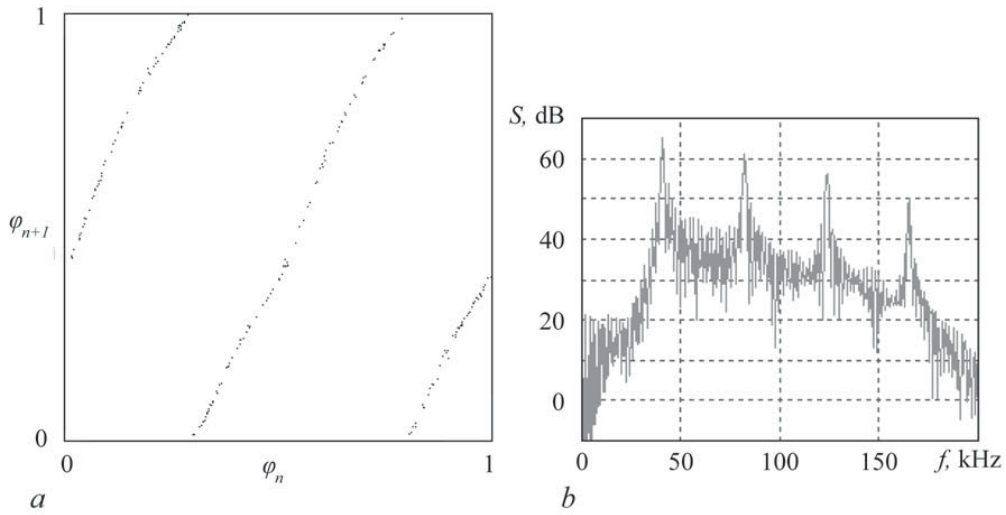

Fig. 12. Diagram illustrating the phase transformation in successive stages of activity (*a*) and the oscillation spectrum in logarithmic scale (*b*) for the oscillator as obtained in the Multisim simulation of the circuit in Fig. 10

To confirm the hyperbolic nature of chaos, it is necessary to make sure that successive stages of activity correspond to phase transformation according to the expanding map. The same as in the previous section, as a phase, we determine the value of the time shift relative to a given reference point normalized to the characteristic period of relaxation oscillations.

To plot a graph for values related to successive stages of activity φ_n and φ_{n+1} we can use the simulation data recorded in a file in the Multisim software for a sufficiently long time with a small sampling step (much smaller than the period of low-amplitude oscillations). The graph obtained by processing these data is shown in Fig. 12, *a*.

Since during the modulation period there is a doubling of the phase variable, the graph consists of branches with a slope coefficient close to 2. Fig. 12, *b* shows the spectrum of the signal generated by the oscillator in logarithmic scale. The spectrum shows obvious similarity with Fig. 9, *a*, which was obtained for the mathematical model in the form of the delay equation (2).

Conclusion

The possibility of rough hyperbolic chaos associated with the Smale–Williams attractor in a system based on the Bonhoeffer–van der Pol oscillator with delayed feedback upon alternating excitation and suppression of activity due to periodic modulation of a parameter is demonstrated by numerical calculations. A circuit of an electronic device that implements the type of dynamics under consideration is developed, and the results of circuit simulation confirming this fact, are presented in the Multisim software.

The obtained results are interesting for constructing electronic chaos generators which are insensitive to parameter variations and noise, as well as from the point of view of possible implementing similar phenomena in different systems, for example, in neurodynamics, namely for neurons with delayed interaction and for analog simulation of such systems.

The considered approach can be regarded as an example for design of various objects with hyperbolic attractors based on systems in which the transfer of the oscillatory excitation between successive stages of activity separated by damping stages is carried out in a resonant manner due to the difference in the frequencies of small and large oscillations by an integer number of times. Structurally,

the scheme is simpler than the previously proposed versions of systems with delay that demonstrate hyperbolic chaos [18, 19], due to the absence of an additional signal source with the frequency close to the frequency of the involved oscillator.

References

1. FitzHugh R. Impulses and physiological states in theoretical models of nerve membrane. *Biophysical Journal*, 1961, vol. 1, no. 6, pp. 445–466.
2. Nagumo J., Arimoto S., Yoshizawa S. An active pulse transmission line simulating nerve axon. *Proceedings of the IRE*, 1962, vol. 50, no. 10, pp. 2061–2070.
3. Izhikevich E.M., FitzHugh R. FitzHugh–Nagumo model. *Scholarpedia*, 2006, vol. 1, no. 9, p. 1349.
4. Izhikevich E.M. Dynamical Systems in Neuroscience: The Geometry of Excitability and Bursting. The MIT Press, Cambridge, MA. 2010.
5. Dmitrichev A.S., Klinshov V.V., Kirillov S.Y., Maslennikov O.V., Shapin D.S., Nekorkin V.I. Nonlinear dynamical models of neurons: Review. *Izvestiya VUZ. Applied Nonlinear Dynamics*, 2018, vol. 26, iss. 4, pp. 5–58 (in Russian).
6. Smale S. Differentiable dynamical systems. *Bulletin of the American mathematical Society*, 1967, vol. 73, no. 6, pp. 747–817.
7. Dynamical Systems with Hyperbolic Behaviour, D.V.Anosov (Ed.). *Encyclopaedia Math. Sci., Dynamical Systems*, vol. 9, Berlin, Springer, 1995.
8. Shilnikov L. Mathematical problems of nonlinear dynamics: A tutorial. *International Journal of Bifurcation and Chaos*, 1997, vol. 7, no. 09, pp. 1953–2001.
9. Sinai Ya.G. The Stochasticity of Dynamical Systems. *Selected Translations. Selecta Math. Soviet.,* 1981, vol. 1, no. 1, pp. 100–119.
10. Katok A. and Hasselblatt B. Introduction to the Modern Theory of Dynamical Systems. *Encyclopedia Math. Appl.*, vol. 54, Cambridge, Cambridge Univ. Press, 1995.
11. Afraimovich V. and Hsu S.-B. Lectures on chaotic dynamical systems. *AMS/IP Stud. Adv. Math.*, 2003, vol. 28.
12. Bonatti C., Díaz L.J., Viana M. Dynamics beyond uniform hyperbolicity: A global geometric and probobalistic perspective. *Encyclopaedia of Mathematical Sciences*, 2005, vol. 102, Mathematical Physics, III, Springer-Verlag, Berlin, p. 2.
13. Ruelle D. Strange attractors. *The Mathematical Intelligencer*, 1980, vol. 2, no. 3, p. 126–137.
14. Andronov A.A., Vitt A.A., Khaikin S.E. Theory of oscillators. Pergamon Press, Oxford, 1966.
15. Pugh C., Peixoto M.M. Structural stability. *Scholarpedia*, 2008, vol. 3, no. 9. 4008.
16. Rabinovich M.I., Trubetskov D.I. Oscillations and Waves in Linear and Nonlinear Systems. Kluwer Academic Publisher, 1989.
17. Kuznetsov S.P. Dynamical chaos and uniformly hyperbolic attractors: From mathematics to physics. *Physics-Uspekhi*, 2011, vol. 54, no. 2, pp. 119–144.
18. Kuznetsov S.P., Ponomarenko V.I. Realization of a strange attractor of the Smale–Williams type in a radiotechnical delay-fedback oscillator. *Technical Physics Letters*, 2008, vol. 34, no. 9, pp. 771–773.
19. Arzhanukhina D.S., Kuznetsov S.P. Robust chaos in autonomous time-delay system. *Izvestiya VUZ. Applied Nonlinear Dynamics*, 2014, vol. 22, no. 2, pp. 36–49 (in Russian).

20. Kuptsov P.V., Kuznetsov S.P. Numerical test for hyperbolicity of chaotic dynamics in time-delay systems. *Phys. Rev. E*, 2016, vol. 94, no. 1, 010201.
21. Kuptsov P.V., Kuznetsov S.P. Numerical test for hyperbolicity in chaotic systems with multiple time delays. *Communications in Nonlinear Science and Numerical Simulation*, 2018, vol. 56, pp. 227–239.
22. Kuznetsov S.P., Sedova Yu.V. Hyperbolic chaos in systems based on FitzHugh–Nagumo model neurons. *Regular and Chaotic Dynamics*, 2018, vol. 23, no. 4, pp. 329–341.
23. Doroshenko V.M., Kruglov V.P., Kuznetsov S.P. Smale–Williams solenoids in a system of coupled Bonhoeffer–van der Pol oscillators. *Russian Journal of Nonlinear Dynamics*, 2018, vol. 14, no. 4, p. 435–451.
24. Kruglov V.P., Kuznetsov S.P. Hyperbolic chaos in a system of two Froude pendulums with alternating periodic braking. *Communications in Nonlinear Science and Numerical Simulation*, 2019, vol. 67, pp. 152–161.
25. Bellman R.E., Cooke K.L. Differential-difference equations. Academic Press, 2012.
26. El'sgol'ts L.E., Norkin S.B. Introduction to the Theory and Application of Differential Equations with Deviating Arguments. Academic Press, 1973.
27. Farmer J. D. Chaotic attractors of an infinite-dimensional dynamical system. *Physica D: Nonlinear Phenomena*, 1982, vol. 4, no. 3, pp. 366–393.
28. Yanchuk S., Giacomelli G. Spatio-temporal phenomena in complex systems with time delays. *Journal of Physics A: Mathematical and Theoretical*, 2017, vol. 50, no. 10, p. 103001.
29. Balyakin A.A., Ryskin N.M. Peculiarities of calculation of the Lyapunov exponents set in distributed self-oscillated systems with delayed feedback. *Izvestiya VUZ. Applied Nonlinear Dynamics*, 2007, vol. 15, no. 6, pp. 3–21 (in Russian).
30. Koloskova A.D., Moskalenko O.I., Koronovskii A.A. A method for calculating the spectrum of Lyapunov exponents for delay systems. *Technical Physics Letters*, 2018, vol. 44, no. 5, pp. 374–377.
31. Sveshnikov A.A. Applied methods of the theory of random functions. Elsevier, 2014.
32. Jenkins G.M., Watts D.G. Spectral analysis and its applications. Holden-Day, 1969.